Quantum Measurement as Marginalization and Nested Quantum Systems

Hans-Andrea Loeliger, *Fellow, IEEE*, and Pascal O. Vontobel, *Senior Member, IEEE*

***Abstract*— In prior work, we have shown how the basic concepts and terms of quantum mechanics relate to factorizations and marginals of complex-valued *quantum mass functions*, which are generalizations of joint probability mass functions. In this paper, using quantum mass functions, we discuss the realization of measurements in terms of unitary interactions and marginalizations. It follows that classical measurement results strictly belong to *local* models, i.e., marginals of more detailed models. Classical variables that are created by marginalization do not exist in the unmarginalized model, and different marginalizations may yield incompatible classical variables. These observations are illustrated by the Frauchiger–Renner paradox, which is analyzed (and resolved) in terms of quantum mass functions. Throughout, the paper uses factor graphs to represent quantum systems/models with multiple measurements at different points in time.**

***Index Terms*— Quantum mechanics, quantum measurement, marginalization, factor graphs.**

I. Introduction

ELEMENTARY quantum mechanics can be roughly summarized to comprise two ingredients as follows.

1) Unitary evolution (UE): between any two points in time, an undisturbed quantum system evolves according to a unitary transformation. This process creates and preserves superpositions and entanglement.
2) Measurements (MEAS): a standard projection measurement changes the state of the system into an eigenstate of the measurement operator, with a probability given by Born's rule. This process eliminates superpositions and entanglement.

The discrepancy between MEAS and UE has been a subject of debate since the early days of quantum mechanics [1]. Much progress has been made in recent years in understanding MEAS as a consequence of interactions with an environment [2]–[7], but this program is far from complete, especially when multiple measurements are involved.

In this paper, we review the derivation of MEAS as an interaction with an enviroment from the perspective of [8]. In that earlier paper, we showed how the basic concepts and terms of quantum mechanics relate to factorizations and marginals of a complex function q, which may be viewed as a generalization of a joint probability mass function. In particular, the joint probability mass function of all measured quantities is a marginal of q.

With hindsight, the function q may be viewed as a simple version of the decoherence functional [9], [10], which has been used in some[1] developments of the consistent-histories approach to quantum mechanics.

In fact, marginalizations of q have long been implicitly used both in tensor networks [12], [13] and in some uses of Feynman path integrals [14]. Marginalization thus deserves to be acknowledged as an independent concept in quantum mechanics on a par with UE. In particular, marginalization is not, in general, unitary, and it allows a transparent treatment of measurement, which is the starting point of this paper.

However, describing MEAS[2] in terms of UE and marginalization has two nontrivial consequences, which have perhaps not been sufficiently emphasized in the literature and which are the main points of this paper.

The first consequence is that the validity of MEAS is not unconditional: in principle (but under extremely unrealistic conditions), measurements can actually be undone.

The second consequence is that classical variables (including classical measurement outcomes) exist only within local models,[3] i.e., marginals of more detailed models. Classical variables that are created by marginalization do not exist in the unmarginalized system, and different marginalizations may yield classical variables that do not coexist. Moreover, the function q can always be refined (i.e., q is a marginal of the refinement) such that any given classical variable in q is no longer classical in the refinement.

Manuscript received February 10, 2019; revised October 6, 2019; accepted December 11, 2019. Date of publication December 23, 2019; date of current version May 20, 2020. The work of P. O. Vontobel was supported in part by a grant from the Research Grants Council of the Hong Kong Special Administrative Region, China, under Project CUHK 14207518.

H.-A. Loeliger is with the Department of Information Technology and Electrical Engineering, ETH Zürich, 8092 Zürich, Switzerland (e-mail: loeliger@isi.ee.ethz.ch).

P. O. Vontobel is with the Department of Information Engineering, The Chinese University of Hong Kong, Hong Kong, and also with the Institute of Theoretical Computer Science and Communications, The Chinese University of Hong Kong, Hong Kong (e-mail: pascal.vontobel@ieee.org).

Communicated by M.-H. Hsieh, Associate Editor for Quantum Information Theory.

Digital Object Identifier 10.1109/TIT.2019.2961377

[1] The decoherence functional is not mentioned in [11].

[2] We mean the standard statistical view of MEAS, which yields probabilities for the outcomes of measurements. We are not concerned with explaining the actual outcomes.

[3] A related notion in the consistent-histories approach is the single-framework rule, which forbids to combine results from incompatible frameworks [11].

The need to relegate classical variables from absolute existence is vividly illustrated by the ingenious Frauchiger–Renner paradox [15] (see also [16], [17]), in which elementary UE and MEAS are shown to yield a plain contradiction. We will carefully analyze the Frauchiger–Renner model using q functions (hence "nested quantum systems" in the title of this paper), and we find all calculations to be in full agreement with those in [15]—except for the actual contradiction, which involves classical variables that do not coexist.[4]

This paper is not concerned with genuine physics (space, time, particles, …), but only with a consistent treatment of projection measurements in terms of marginalized unitary interactions. We also note that this paper appears to be rather closely related to the consistent-histories approach [9]–[11]. However, our starting point is quite different, and the elaboration of the pertinent connections is beyond the scope of this paper.

As in [8], we heavily use factor graphs to specify functions q and to reason about them. A brief summary of this notation is given in Section II; for a more detailed exposition, we refer to [8].

Beyond Section II, this paper is structured as follows. In Section III, we formally state some properties of quantum mass functions q and related concepts, including marginals and classical variables. In Section IV, we review the foundations of measurement by marginalized interaction and its implications for the validity of MEAS. In Section V, we analyze the Frauchiger–Renner paradox.

As in [8], we will use standard linear algebra notation rather than the bra-ket notation of quantum mechanics. The Hermitian transpose of a complex matrix A will be denoted by $A^{\mathsf{H}} = \overline{A^{\mathsf{T}}}$, where A^{T} is the transpose of A and $\overline{A}$ is the componentwise complex conjugate of A. An identity matrix will be denoted by I. We will often view a matrix A as a function $A(x, y)$, where x is the row index of A and y is the column index of A. In this notation, $A(\cdot, y)$ denotes column y of A.

II. FACTOR GRAPHS AND QUANTUM MASS FUNCTIONS

As shown in [8], joint probabilities of outcomes $y_1, \dots, y_n$ of multiple measurement in quantum mechanics (at different points in time) can be written as

$$p(y_1, \dots, y_n) = \sum_{x_1, \dots, x_m} q(y_1, \dots, y_n, x_1, \dots, x_m), \qquad (1)$$

where the sum is over all possible values[5] of $x_1, \dots, x_m$ and where q is a complex-valued function that allows natural factorizations in terms of unitary evolutions and measurements. (Detailed explanations of (1) will be given below.) Such functions q may be viewed as generalizations of joint probability mass functions and will in this paper be called *quantum mass functions.*

[4]Assumption C of [15] presumes the absolute existence of measurement results and does not hold in this paper.

[5] In this paper (as in [8]), all variables take values in finite sets. The generalization to more general variables is conceptually straightforward but raises technical issues outside the scope of this paper.

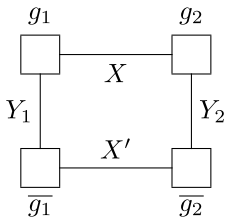

Fig. 1. Factor graph of (2).

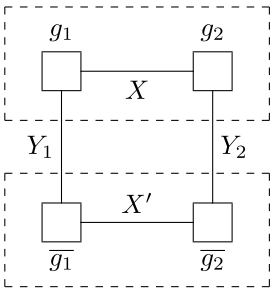

Fig. 2. The dashed boxes represent the two sums in (3).

Such quantum mass functions have some commonalities with quasi-probability distributions that have a long tradition in quantum mechanics going back Wigner–Weyl representations. (See also Appendix B of [8], where q functions are transformed into Wigner–Weyl representations.) However, quantum mass functions are complex valued.

Functions q as in [8] are implicitly represented in tensor networks, cf. [12], [13] and [8, Appendix A]. However, using tensor networks to represent *joint* probabilities of multiple measurements at different points of time does not seem to be documented in the literature.

As mentioned in Section I, the function q may actually be viewed as a simple version of the decoherence functional [9], [10].

A. Forney Factor Graphs

As in [8], we use Forney factor graphs [18] (also known as normal factor graphs) to represent factorizations of functions. For a detailed exposition to this graphical notation we refer to [8]. In this section, we just give a brief summary of it.

For example, Fig. 1 represents a function

$$q(y_1, y_2, x, x') = g_1(y_1, x) g_2(y_2, x) \overline{g_1(y_1, x')}\, \overline{g_2(y_2, x')}, \qquad (2)$$

where g_1 and g_2 are arbitrary complex-valued functions with suitable domains. (Variables like "X" in Fig. 1 are normally capitalized, except when used as argument of functions as in (2).) Note that

$$\sum_{x, x'} q(y_1, y_2, x, x')$$
$$= \Big(\sum_x g_1(y_1, x) g_2(y_2, x) \Big) \overline{\Big(\sum_{x'} g_1(y_1, x') g_2(y_2, x') \Big)} \qquad (3)$$
$$= \Big| \sum_x g_1(y_1, x) g_2(y_2, x) \Big|^2 \qquad (4)$$

is real and nonnegative. If (4) is not identically zero, then, with suitable scaling, (4) is a probability mass function over

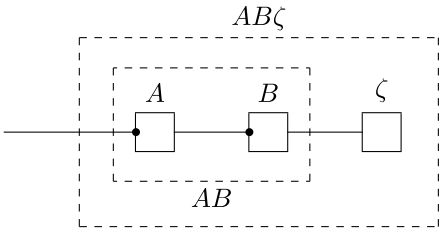

Fig. 3. Factor graph representation of matrix multiplication (AB) and matrix-times-vector multiplication. The row index of a matrix is marked by a dot. (Marking the row index of the column vector ζ in this way is optional.)

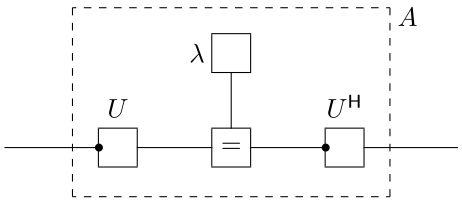

Fig. 4. Factor graph of (5).

y_1 and y_2 and (2) is a quantum mass function (as will be defined below).

The factor graph notation is intimately related to the idea of opening and closing boxes, such as the two dashed boxes in Fig. 2. The *exterior function* of a box is defined to be the sum, over its internal variables, of the product of its internal factors. For example, the exterior function of the upper dashed box in Fig. 2 is the first sum in (3). Closing a box means to replace the box by a single node that represents the exterior function of the box. Opening a box means the converse operation of expanding a node into a factor graph of its own.

A matrix may be viewed as a function of two variables: the row index and the column index. Matrix multiplication can then be represented as exemplified in Fig. 3, which shows the product $AB\zeta$ of matrices A and B and a vector ζ of suitable dimensions. Closing and opening boxes in factor graphs may thus be viewed as generalizations of matrix multiplication and matrix factorization, respectively.

Fig. 3 also illustrates the pivotal property of factor graphs that opening or closing an inner box inside some outer box does not change the exterior function of the outer box.

Finally, Fig. 4 shows the decomposition of a positive semidefinite matrix A according to the spectral theorem as

$$A = U\Lambda U^{\mathsf{H}}, \tag{5}$$

where U is unitary and Λ is diagonal with diagonal vector λ. The node labeled "=" in Fig. 4 represents the equality constraint function

$$f_{=}(x_1, x_2, x_3) = \begin{cases} 1, & \text{if } x_1 = x_2 = x_3 \\ 0, & \text{otherwise.} \end{cases} \tag{6}$$

The equality constraint function with any number (≥ 2) of arguments is defined by the obvious generalization of (6). The equality constraint function with two arguments can represent an identity matrix; the equality constraint function with three or more arguments can represent branching points or, equivalently, creates copies of a variable as in Fig. 4.

B. Factor Graphs of Quantum Systems

Fig. 5 shows the factor graph of a quantum mass function of an elementary quantum system, consisting of an initial density matrix, a unitary evolution, a projection measurement with result Y, and a termination. The symbols U_0, U_1, and B denote unitary matrices in $\mathbb{C}^{M\times M}$ (i.e., our Hilbert space is $\mathbb{C}^M$). All variables in Fig. 5 (including $X_0, X_0', \ldots, X_4, X_4'$ and Y) take values in $\{1, \ldots, M\}$, i.e., they index rows and columns of matrices in $\mathbb{C}^{M\times M}$.

The initial state is a mixture, with mixing probabilities $p(x_0)$. The exterior function of the dashed box on the left-hand side in Fig. 5 is the initial density matrix

$$\rho(x_1, x_1') = \big(U_0 \Lambda U_0^{\mathsf{H}}\big)(x_1, x_1'), \tag{7}$$

where $\Lambda \in \mathbb{C}^{M\times M}$ is a diagonal matrix with diagonal elements $\{p(x_0)\colon x_0 = 1, \ldots, M\}$, cf. Fig. 4. The measurement operator (the second dashed box in Fig. 5) represents a projection measurement with respect to a basis consisting of the columns of B. The termination (the equality constraint between X_4 and X_4'), summarizes the future beyond the period of interest.

Two illustrative regroupings of Fig. 5 are shown in Figs. 6 and 7. The exterior function of the dashed box on the right-hand side in Fig. 6 is the constant 1; this box can thus be omitted without changing $p(y)$. The exterior function of the dashed box on the left-hand side in Fig. 6 is the probability mass function

$$p(y) = \sum_{x_0=1}^{M} \big|B(\cdot, y)^{\mathsf{H}} U_1 U_0(\cdot, x_0)\big|^2 p(x_0), \tag{8}$$

where $B(\cdot, y)$ denotes column y of the matrix B.

In Fig. 7, the exterior function of the outer dashed box is the post-measurement density matrix. Note that this post-measurement density matrix has the same structure as the initial density matrix in Fig. 5, with $p(x_0)$ replaced by $p(y)$ und U_0 replaced by B. Note also that the termination (i.e., the identity matrix between X_4 and X_4') is required in order to turn the post-measurement density matrix into a quantum mass function.

Fig. 8 shows a quantum mass function of a general quantum system with two measurements, with results Y_1 and Y_2. (The generalization to any number of measurements is obvious.) The matrices U_0, U_1, U_2, B_1, and B_2 are unitary. The rows of U_0, the columns of U_2, and both rows and columns of U_1 are indexed by a pair of variables. The two measurements are projection measurements as in Fig. 5, but involve only a subset of the variables.

It is proved in [8] that this graphical approach correctly represents standard quantum mechanics. In particular, the exterior function of Fig. 8, and of its generalization to any number n of observations $Y_1, \ldots, Y_n$, is the correct joint probability mass function $p(y_1, y_2)$ and $p(y_1, \ldots, y_n)$, respectively.

Note that the upper half and the lower half of Fig. 8 (and of Fig. 5) are mirror images of each other, which makes these factor graphs somewhat redundant. This redundancy is eliminated in the more compact factor graph representation proposed in [19], which has other advantages as well. However, the present paper is much concerned with the interactions of the two

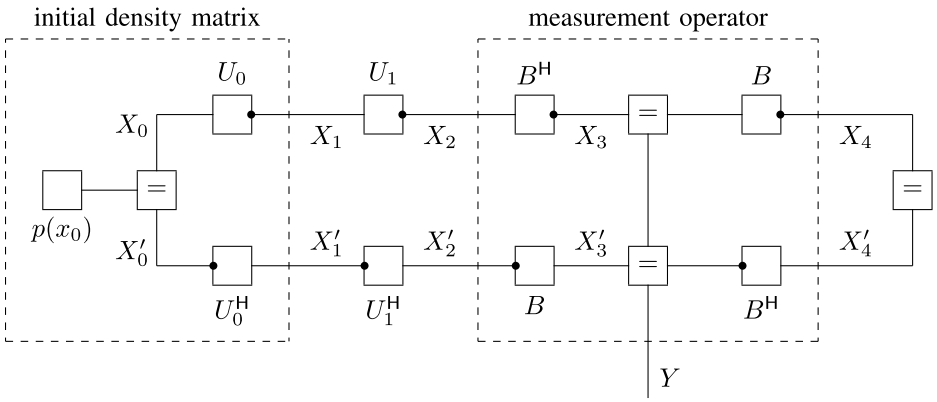

Fig. 5. Factor graph of an elementary quantum system: initial density matrix, unitary evolution, projection measurement with result Y, and termination.

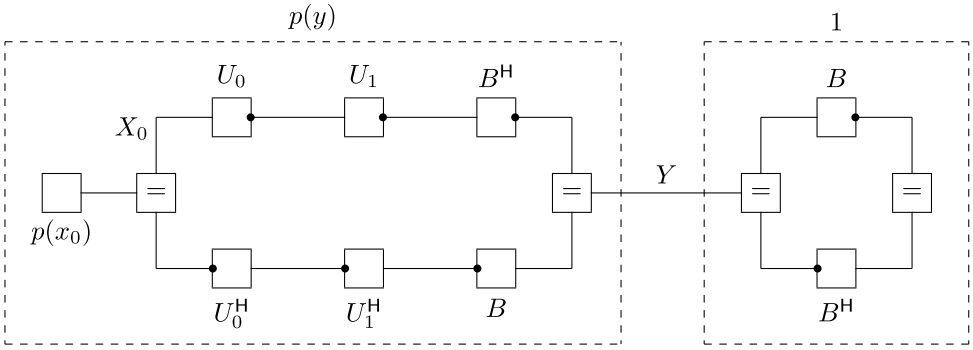

Fig. 6. A regrouping of Fig. 5 (with an immaterial rearrangement of the equality constraints). The dashed box on the right reduces to a neutral factor that can be omitted.

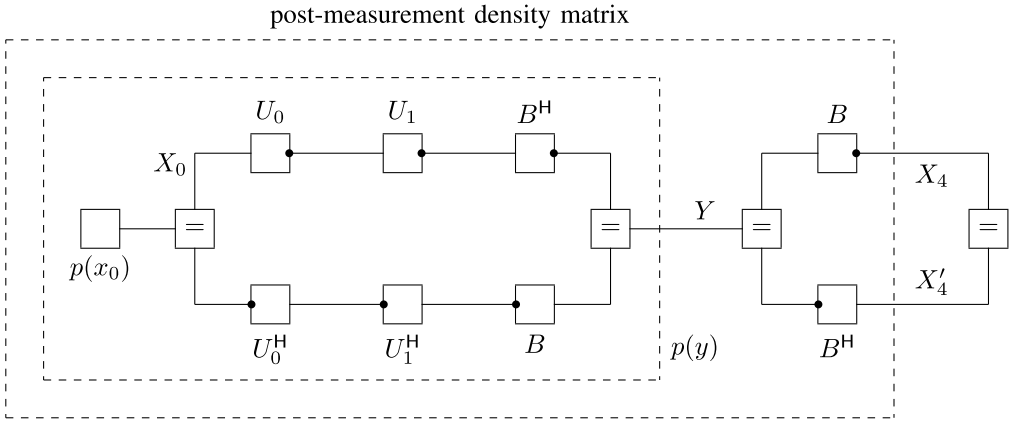

Fig. 7. Another regrouping of Fig. 5 that displays the post-measurement density matrix.

mirror halves, and these interactions are more obvious in the redundant version.

In particular, every projection measurement involves an equality constraint between two mirror variables, and these equality constraints are the chief objects of study in this paper.

If Y_2 in Fig. 8 is unknown, the dashed box in Fig. 9 reduces to an identity matrix, cf. [8, Section II.C]. Likewise, the dashed box in Fig. 8 reduces to an identity matrix that summarizes arbitrary future unitary evolutions and measurements with unknown results, cf. Proposition 2 of [8].

Finally, Fig. 10 illustrates the characteristic idempotence of projection measurements: a second projection measurement after an identical first projection measurement has the same result and no additional effect.

III. On Quantum Mass Functions and Quantum Variables

We now formally state some properties of quantum mass functions and related concepts as exemplified by Figs. 5 and 8. The terms and concepts that we are going to use (PSD kernels, classicality,[6] ...) are standard for density matrices, but we adapt them here to quantum mass functions of many variables involving multiple measurements at different points of time.

[6]A diagonal density matrix is sufficient, but not necessary for classicality as defined in Section III-D, and joint classicability as in Section III-D appears to be a new concept.

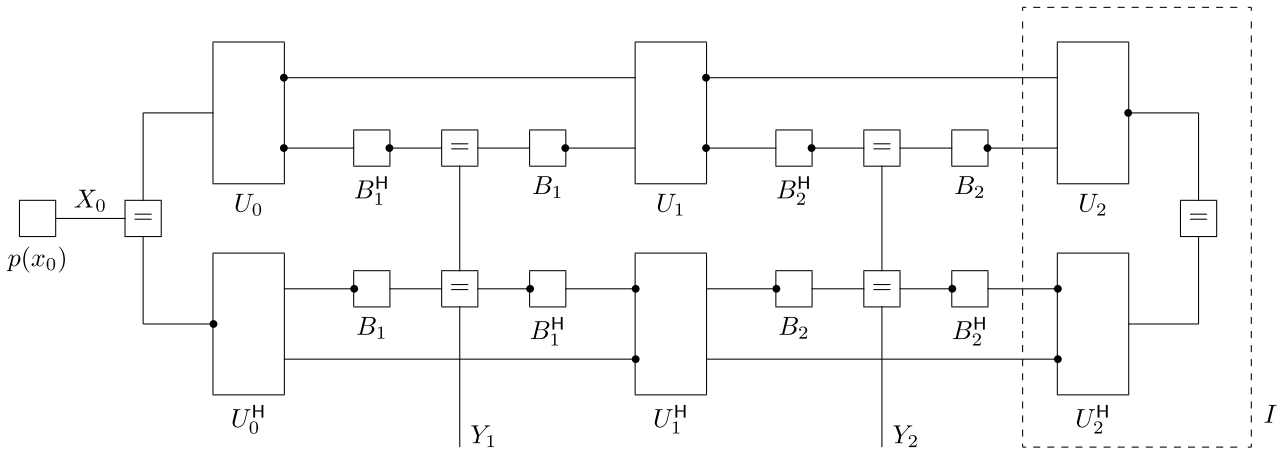

Fig. 8. Factor graph of a general quantum system with two partial projection measurements. The generalization to any number of measurements is obvious.

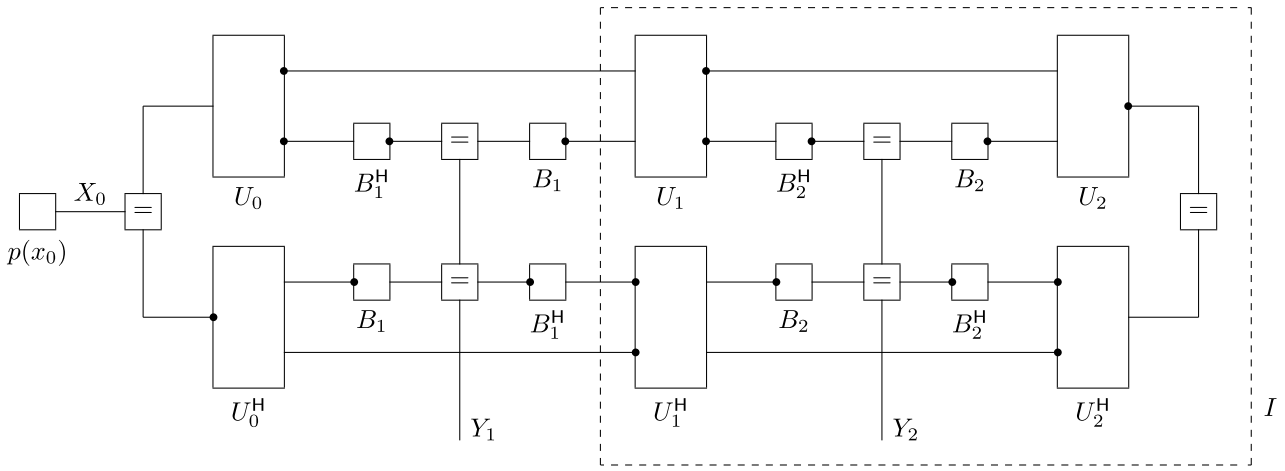

Fig. 9. If the result Y_2 in Fig. 8 is not known, the dashed box reduces to an identity matrix.

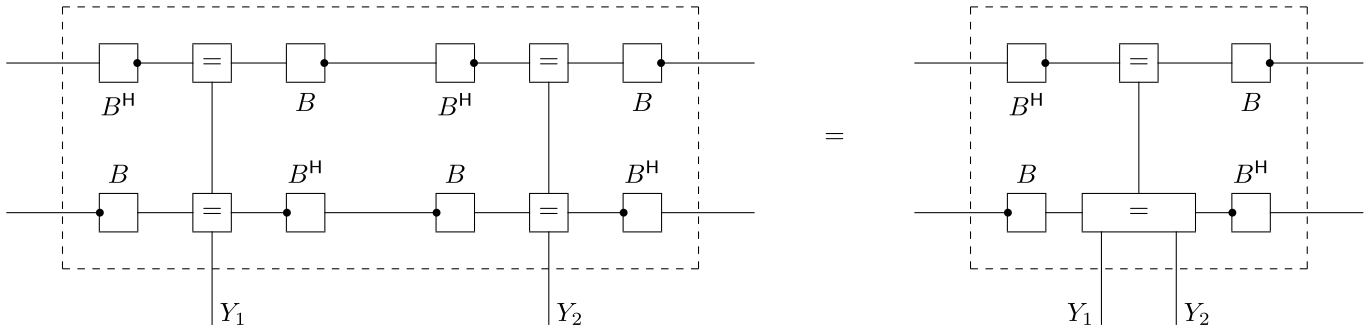

Fig. 10. Two identical projection measurements, one immediately following the other, reduce to a single projection measurement with two identical results. (The dashed boxes left and right have the same exterior function.)

A. Background: PSD Kernels

A *positive semidefinite (PSD) kernel* with *finite*[7] domain $\mathcal{A} \times \mathcal{A}$ is a function $q : \mathcal{A} \times \mathcal{A} \to \mathbb{C}$ such that

$$q(x, x') = \overline{q(x', x)} \tag{9}$$

and

$$\sum_{x \in \mathcal{A}} \sum_{x' \in \mathcal{A}} \overline{g(x)} q(x, x') g(x') \geq 0 \tag{10}$$

for every function $g : \mathcal{A} \to \mathbb{C}$. In other words, the square matrix with index set $\mathcal{A}$ and entries $q(x, x')$ is Hermitian and positive semidefinite.

Clearly, any function of the form

$$q(x, x') = f(x)\overline{f(x')} \tag{11}$$

is a PSD kernel.

[7]In this paper, we consider only PSD kernels and quantum mass functions with *finite* domain, cf. footnote 5.

By the spectral theorem, a PSD kernel with finite domain $\mathcal{A} \times \mathcal{A}$ can be written as

$$q(x, x') = \sum_{\xi \in \mathcal{A}} u(x, \xi) \lambda(\xi) \overline{u(x', \xi)}, \tag{12}$$

where the square matrix u with index set $\mathcal{A}$ and entries $u(x, \xi)$ is unitary and $\lambda(\xi)$ is real with $\lambda(\xi) \geq 0$ for all $\xi \in \mathcal{A}$.

If q and $\tilde{q}$ are PSD kernels with finite domain $\mathcal{A} \times \mathcal{A}$, then both their sum $q(x, x') + \tilde{q}(x, x')$ and their product $q(x, x')\tilde{q}(x, x')$ are PSD kernels. (For the sum, the proof is obvious; for the product, (10) follows from the Schur product theorem, but can easily be proved directly using (12).)

B. Quantum Mass Functions and Quantum Variables

Definition 1. A *quantum mass function* with finite domain is a complex-valued function $q(x, x'; y)$ such that, for every y, $q(x, x'; y)$ is a PSD kernel with finite domain and

$$\sum_y \sum_x \sum_{x'} q(x, x'; y) = 1. \tag{13}$$

A *simple quantum mass function* (SQMF) with finite domain is a complex-valued PSD kernel $q(x, x')$ with finite domain such that

$$\sum_x \sum_{x'} q(x, x') = 1. \tag{14}$$

□

Note that the sums in (13) and (14) run over the whole domain of q.

Figs. 5–9 represent quantum mass functions, where the third argument is used for measurement results such as Y in Fig. 5. In this paper, however, we will henceforth consider only SQMFs, which simplifies the notation. Measurement results will be expressed in terms of the involved quantum variables (such as X_3 and X_3' in Fig. 5).

The domain of an SQMF is a finite set

$$\Omega = \mathcal{A} \times \mathcal{A}. \tag{15}$$

In this paper, the set $\mathcal{A}$ is usually a product of finite sets, i.e., $\mathcal{A} = \mathcal{A}_1 \times \mathcal{A}_2 \times \cdots \times \mathcal{A}_N$. With a slight abuse of notation, we then write (15) also as

$$\Omega = \mathcal{A}_1^2 \times \cdots \times \mathcal{A}_N^2. \tag{16}$$

Elements of Ω will be called *configurations* and will be denoted both by (x, x') and by $\big((x_1, x_1'), \ldots, (x_N, x_N')\big)$ with $x = (x_1, \ldots, x_N)$ and $x' = (x_1', \ldots, x_N')$. The domain Ω will also be called the *configuration space*. A configuration $(x, x') \in \Omega$ is called *valid* if $q(x, x') \neq 0$.

A configuration (x, x') may be viewed as a pair of Feynman paths, where x is a path in one half of the factor graph and x' is a path in the other half (the mirror part) of the factor graph.

A *quantum variable* is a function

$$X_k \colon \Omega \to \mathcal{A}_k \colon \big((x_1, x_1'), \ldots, (x_N, x_N')\big) \mapsto x_k \tag{17}$$

or

$$X_k' \colon \Omega \to \mathcal{A}_k \colon \big((x_1, x_1'), \ldots, (x_N, x_N')\big) \mapsto x_k'. \tag{18}$$

The two quantum variables (17) and (18) are called *conjugates* of each other.

C. Marginals and Refinements

A *marginal* of an SQMF with domain (16) is a function

$$\begin{aligned} &\mathcal{A}_{k_1}^2 \times \cdots \times \mathcal{A}_{k_L}^2 \to \mathbb{C} \colon \big((x_{k_1}, x_{k_1}'), \ldots, (x_{k_L}, x_{k_L}')\big) \\ &\quad \mapsto \sum_{x_{k_{L+1}}, x_{k_{L+1}}'} \cdots \sum_{x_{k_N}, x_{k_N}'} q\big((x_1, x_1'), \ldots, (x_N, x_N')\big), \end{aligned} \tag{19}$$

where $k_1, \ldots, k_L$ (with $1 \leq L < N$) are L different indices in $\{1, \ldots, N\}$, $k_{L+1}, \ldots, k_N$ are the remaining indices, and the sums run over all pairs $(x_{k_\ell}, x_{k_\ell}') \in \mathcal{A}_{k_\ell}^2$, $\ell = L+1, \ldots, N$.

Proposition 1. A marginal of an SQMF is itself an SQMF. □

The proof is given below.

An SQMF q is said to be a *refinement* of another quantum mass function $\breve{q}$ if $\breve{q}$ is a marginal of q.

Mimicking a standard convention for probability mass functions, the function (19) will be denoted by $q\big((x_{k_1}, x_{k_1}'), \ldots, (x_{k_L}, x_{k_L}')\big)$, if this is possible without confusion. For example, $q\big((x_1, x_1')\big)$ denotes the marginal

$$\begin{aligned} &\mathcal{A}_1^2 \to \mathbb{C} \colon \\ &\quad (x_1, x_1') \mapsto \sum_{x_2, x_2'} \cdots \sum_{x_N, x_N'} q\big((x_1, x_1'), \ldots, (x_N, x_N')\big). \end{aligned} \tag{20}$$

Proof of Proposition 1: Without loss of essential generality, we consider only the marginal $q\big((x_1, x_1')\big)$ of a given SQMF $q\big((x_1, x_1'), (x_2, x_2')\big)$. We have to verify that $q\big((x_1, x_1')\big)$ satisfies (9), (10), and (14).

As for Condition (9), we have

$$\begin{aligned} q\big((x_1, x_1')\big) &= \sum_{x_2, x_2'} q\big((x_1, x_1'), (x_2, x_2')\big) && (21) \\ &= \sum_{x_2, x_2'} \overline{q\big((x_1', x_1), (x_2', x_2)\big)} && (22) \\ &= \overline{\sum_{x_2, x_2'} q\big((x_1', x_1), (x_2, x_2')\big)} && (23) \\ &= \overline{q\big((x_1', x_1)\big)}. && (24) \end{aligned}$$

As for Condition (10), we have

$$\begin{aligned} &\sum_{x_1, x_1'} \overline{g(x_1)} q\big((x_1, x_1')\big) g(x_1') \\ &\quad = \sum_{x_1, x_1'} \overline{g(x_1)} g(x_1') \sum_{x_2, x_2'} q\big((x_1, x_1'), (x_2, x_2')\big) && (25) \\ &\quad = \sum_{x_1, x_1'} \sum_{x_2, x_2'} \overline{g(x_1)} q\big((x_1, x_1'), (x_2, x_2')\big) g(x_1') && (26) \\ &\quad \geq 0. && (27) \end{aligned}$$

Finally, Condition (14) is obvious:

$$\begin{aligned} \sum_{x_1, x_1'} q\big((x_1, x_1')\big) &= \sum_{x_1, x_1'} \sum_{x_2, x_2'} q\big((x_1, x_1'), (x_2, x_2')\big) && (28) \\ &= 1. && (29) \end{aligned}$$

■

D. Classical and Classicable Variables

Definition 2. Let q be an SQMF with domain (16). A quantum variable X_k or X'_k as in (17) or (18), respectively, is called *classical with* q if $X_k = X'_k$ in every valid configuration of q. □

Note that projection measurements as in Figs. 5 and 8 create classical variables by an equality constraint between conjugate quantum variables. In Section IV, we will discuss the creation of such equality constraints by marginalized unitary interactions.

Proposition 2. If X_k is classical with q, then it is classical with every marginal of q in which it appears. □

(The proof is obvious.) However, X_k need not be classical with refinements of q, hence the qualifier "with q" in the definition.

Proposition 3. Let q be an SQMF with domain (16). If the quantum variables $X_1, \ldots, X_N$ are all classical with q, then q is a probability mass function. □

Proof: Assume that $X_1, \ldots, X_N$ are all classical with q, i.e., $q(x, x') = 0$ for $x \neq x'$. We also have $q(x, x) \in \mathbb{R}$ by (9). It remains to prove that $q(x, x) \geq 0$ for all x. Indeed, using (10), we have

$$q(\xi, \xi) = \sum_x \sum_{x'} \overline{f_=(x, \xi)} q(x, x') f_=(x', \xi) \tag{30}$$

$$\geq 0. \tag{31}$$

■

Classicality as in Definition 2 is rather fragile: it may disappear with refinements of q. The following concept is more robust.

Definition 3. Let q be an SQMF with domain (16). A quantum variable X_k is called *classicable* if the marginal $q(x_k, x'_k)$ satisfies

$$q(x_k, x'_k) = 0 \quad \text{for } x_k \neq x'_k. \tag{32}$$

More generally, a set of quantum variables $X_{k_1}, \ldots, X_{k_L}$ is called *jointly classicable* if

$$q\big((x_{k_1}, x'_{k_1}), \ldots, (x_{k_L}, x'_{k_L})\big) = 0 \tag{33}$$

unless $x_{k_1} = x'_{k_1}$, ..., $x_{k_L} = x'_{k_L}$. □

The following two propositions are obvious.

Proposition 4. For a given SQMF q, all variables that are classical with q are jointly classicable. □

Proposition 5. For a given SQMF q, if $X_{k_1}, \ldots, X_{k_L}$ are jointly classicable, then these quantum variables are joinly classicable in every refinement of q and classical with the marginal $q\big((x_{k_1}, x'_{k_1}), \ldots, (x_{k_L}, x'_{k_L})\big)$. □

For example, consider the variables in Fig. 11, where U_1 and U_2 are unitary matrices. In order to avoid trivial special cases, we assume that all entries of these two matrices have magnitude strictly smaller than 1. The variables X_0 and X_2 are obviously classical. The variables X_0 and X_1 are jointly classicable as illustrated in Fig. 12. The variables X_1 and X_2 are jointly classicable if and only if $p(x_0)$ is uniform. The variables X_0, X_1, X_2 are not jointly classicable.

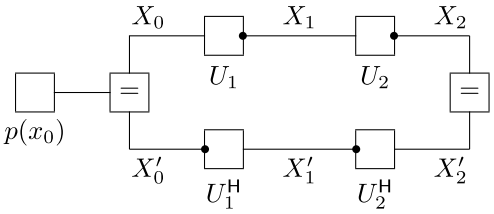

Fig. 11. The example at the end of Section III-D.

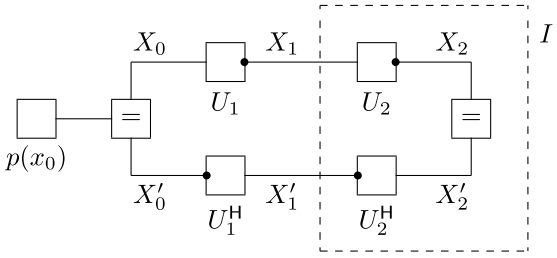

Fig. 12. Closing the dashed box makes X_1 classical.

IV. Classicality and Measurement by Marginalization

So far, we have treated measurements as an undefined primitive, in full agreement with the standard axioms of quantum mechanics. We now address the realization of projection measurements by means of marginalization, and its consequences for the validity of MEAS.

Recall from Figs. 5, 8, and 10 that a projection measurement can be represented as in Fig. 13 (right),[8] where the columns of the unitary matrix B define the basis of the measurement. In particular, a projection measurement involves an equality constraint between two conjugate quantum variables, which creates a classical variable ζ that is the effective result of the measurement. (As in Section III, we here do not use a copy of ζ like Y, Y_1, Y_2 in Figs. 5, 8, and 10 for the classical result.)

Consider the realization of Fig. 13 (right) as in Fig. 13 (left), where $\tilde{U}$ is a unitary matrix and where the variables ξ and $\tilde{\xi}$ belong to a secondary quantum system (a particle or an environment) that interacts once with the system of interest. Fig. 13 (left) realizes the projection measurement[9] in Fig. 13 (right) if and only if the exterior function of the dashed box (left) equals the exterior function of the dashed box (right).

We next note that it suffices to study the case where B is an identity matrix: if, for some $\tilde{U}$, Fig. 13 (left) realizes a projection measurement with $B = I$, an obvious modification of $\tilde{U}$ realizes a projection measurement for any unitary matrix B.

[8]The factor graphs in Figs. 13–16 (and in Fig. 10) do not show quantum mass functions, but building blocks (boxes) for use in a (larger) factor graph of some quantum mass function.

[9]It is well known that *any* measurement (including, but not limited to, projection measurements) can be represented as in Fig. 13 (left), cf. [20], [8, Section V.C].

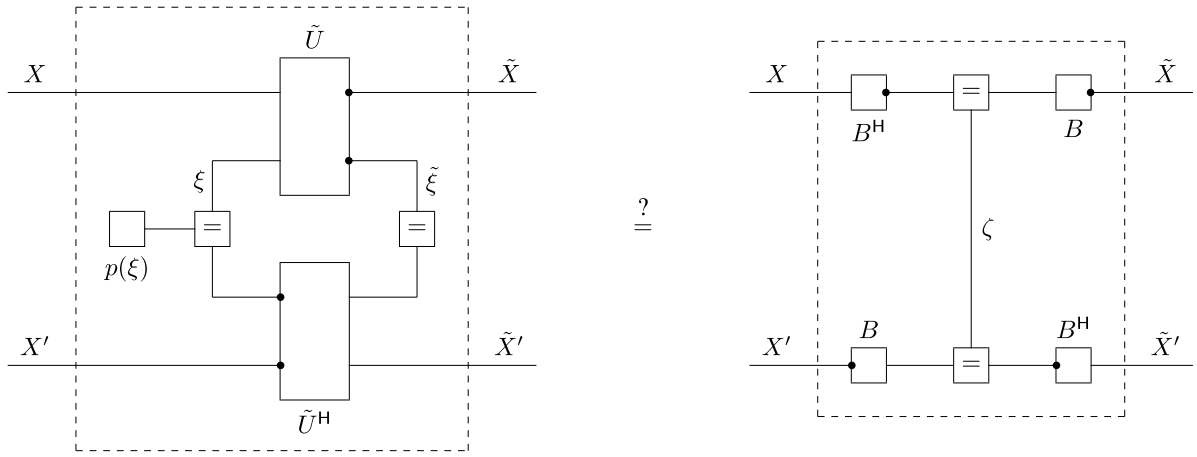

Fig. 13. A marginalized unitary interaction (left) may amount to a projection measurement (right).

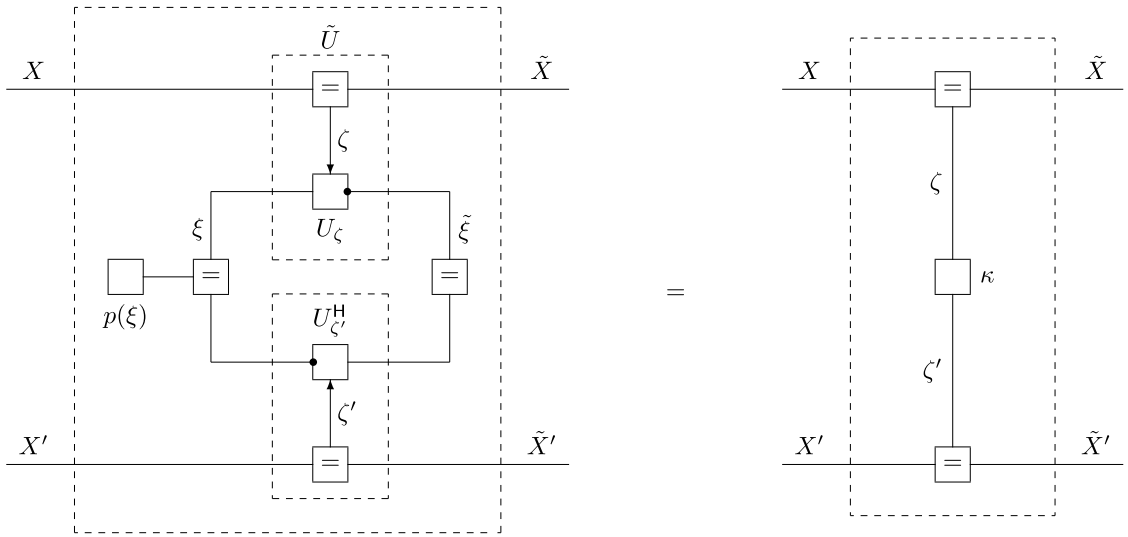

Fig. 14. A class of unitary interactions as in Fig. 13 (left) yielding (38) and (44). The function κ is defined in Fig. 15. A projection measurement (with $B = I$) results if and only if $\kappa(\zeta, \zeta') = f_{=}(\zeta, \zeta')$.

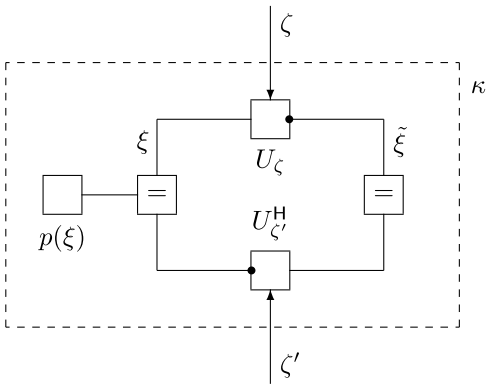

Fig. 15. The function κ appearing in Fig. 14 (right) and in Eq. (36) is the exterior function of the dashed box.

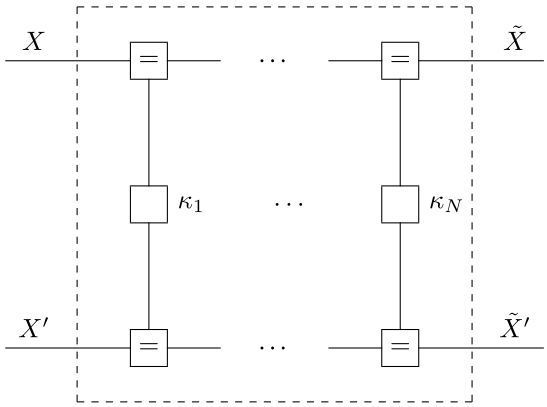

Fig. 16. N interactions as in Fig. 14, summarized by $\kappa_1, \ldots, \kappa_N$, have the same effect as a single such interaction with κ as in (45).

We now specialize (for the rest of this section) to the situation shown in Fig. 14. Fig. 14 (left) shows a special case of Fig. 13 (left), as will be discussed below. Clearly, Fig. 14 (left) can be represented as in Fig. 14 (right) with κ as in Fig. 15 (i.e., the exterior function of the outer dashed box in Fig. 14 (left) equals the exterior function of the dashed box in Fig. 14 (right)). Note that ζ and ζ' are simply copies of X and X', respectively. It is then obvious from Fig. 14 (right)

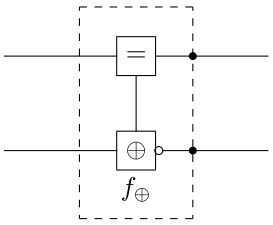

Fig. 17. A unitary matrix $\tilde{U}$ as in Section IV-A. The tiny circle marks an argument of $f_\oplus$ with a negative sign as in (42). For $M = 2$, this matrix is a quantum-controlled NOT gate.

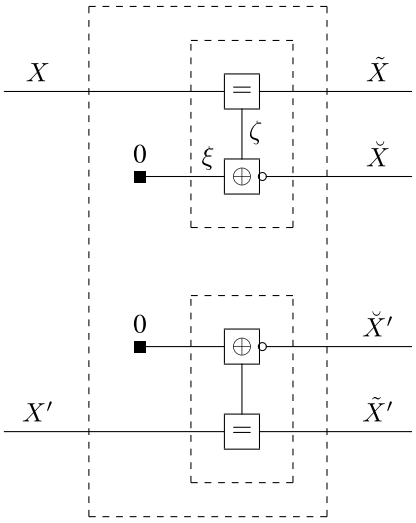

Fig. 18. Creating a maximally entangled copy $\breve{X}$ of X using the circuit of Fig. 17. The small filled boxes indicates a fixed known value (in this case zero).

that Fig. 14 realizes a projection measurement with $B = I$ if and only if $\kappa(\zeta, \zeta') = f_=(\zeta, \zeta')$.

We now turn to the details of Fig. 14 (left), where U_ζ and $U_{\zeta'}$ are unitary matrices that depend on ζ and ζ', respectively (i.e., U_ζ and $U_{\zeta'}$ effectively depend on X and X', respectively). The inner dashed boxes in Fig. 14 (left) realize the unitary[10] matrices $\tilde{U}$ and $\tilde{U}^{\mathsf{H}}$ in Fig. 13, where

$$\tilde{U}\big((\tilde{x}, \tilde{\xi}), (x, \xi)\big) = \begin{cases} U_x(\tilde{\xi}, \xi), & \text{if } x = \tilde{x} \\ 0, & \text{otherwise} \end{cases} \tag{34}$$

$$= \sum_\zeta \begin{cases} U_\zeta(\tilde{\xi}, \xi), & \text{if } \zeta = x = \tilde{x} \\ 0, & \text{otherwise.} \end{cases} \tag{35}$$

The function κ in Fig. 14 (right) and Fig. 15 is

$$\kappa(\zeta, \zeta') \triangleq \sum_\xi \sum_{\tilde{\xi}} p(\xi) U_{\zeta'}^{\mathsf{H}}(\xi, \tilde{\xi}) U_\zeta(\tilde{\xi}, \xi) \tag{36}$$

$$= \sum_\xi p(\xi) U_{\zeta'}(\cdot, \xi)^{\mathsf{H}} U_\zeta(\cdot, \xi). \tag{37}$$

It follows that

$$\kappa(\zeta, \zeta') = 1 \quad \text{if } \zeta = \zeta'. \tag{38}$$

[10]The matrices $\tilde{U}$ in Fig. 14 (left) are easily verified to be unitary by adapting the graphical proof of Fig. 46 of [8].

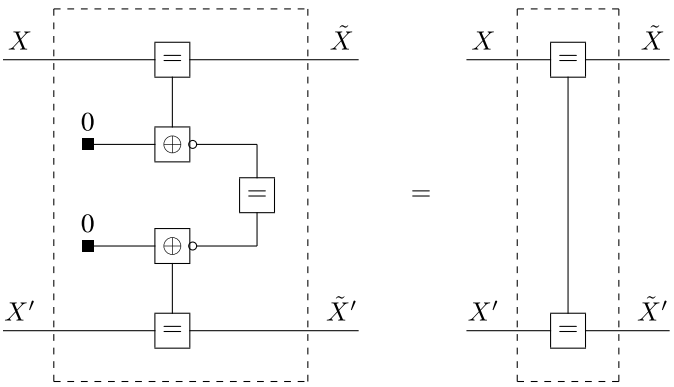

Fig. 19. Measurement by a marginalized copy.

(See (44) for the off-diagonal values in the general case.) Thus Fig. 14 amounts to a projection measurement if and only if

$$\kappa(\zeta, \zeta') = 0 \quad \text{if } \zeta \neq \zeta'. \tag{39}$$

Three different ways to achieve (39) will be discussed below.

A. One-Shot Projection Measurement

A mathematically direct, but somewhat unphysical, realization of a projection measurement is obtained with a unitary matrix U_ζ satisfying the following condition: if any two of the three variables $\zeta, \xi, \tilde{\xi}$ are set to arbitrary values, then

$$U_\zeta(\xi, \tilde{\xi}) = \begin{cases} 1, & \text{for exactly one value of the third variable} \\ 0, & \text{otherwise.} \end{cases} \tag{40}$$

Writing (36) as

$$\kappa(\zeta, \zeta') = \sum_\xi \sum_{\tilde{\xi}} p(\xi) \overline{U_{\zeta'}(\tilde{\xi}, \xi)} U_\zeta(\tilde{\xi}, \xi) \tag{41}$$

and inserting (40) into (41), it is easily verified that (39) holds.

An example of such a matrix is

$$U_\zeta(\xi, \tilde{\xi}) = f_\oplus(\zeta, \xi, -\tilde{\xi}) \tag{42}$$

with

$$f_\oplus(\zeta, \xi, \tilde{\xi}) \triangleq \begin{cases} 1, & \text{if } \zeta + \xi + \tilde{\xi} = 0 \mod M \\ 0, & \text{otherwise,} \end{cases} \tag{43}$$

where all variables are assumed to take values in $\{0, 1, \ldots, M-1\}$, cf. Fig. 17 and [8, Section VI.A]. For $M = 2$, the resulting matrix $\tilde{U}$ is a quantum-controlled NOT gate.

B. Classicality From Multiple Interactions

Assuming $p(\xi) > 0$ for all ξ, it follows from (37) that

$$|\kappa(\zeta, \zeta')| < 1 \quad \text{if } U_\zeta \neq U_{\zeta'}. \tag{44}$$

This can be used to realize a projection measurement by means of multiple interactions as in Fig. 14, each with its own set of unitary matrices $\{U_\zeta\}$. Clearly, N such interactions, resulting

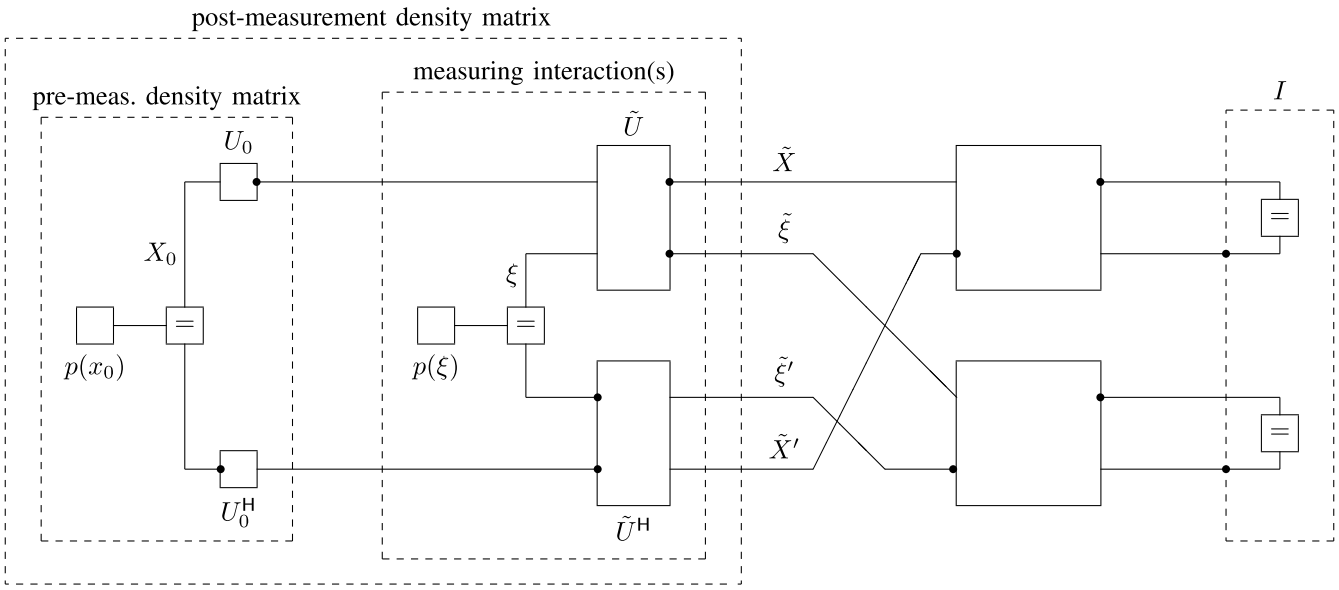

Fig. 20. The Separation Condition: after the measuring interaction(s) $\tilde{U}$, the measuring system must not again interact with the system of interest within the period of interest. The period of interest ends with the terminating identity matrix, which summarizes an arbitrary unknown future.

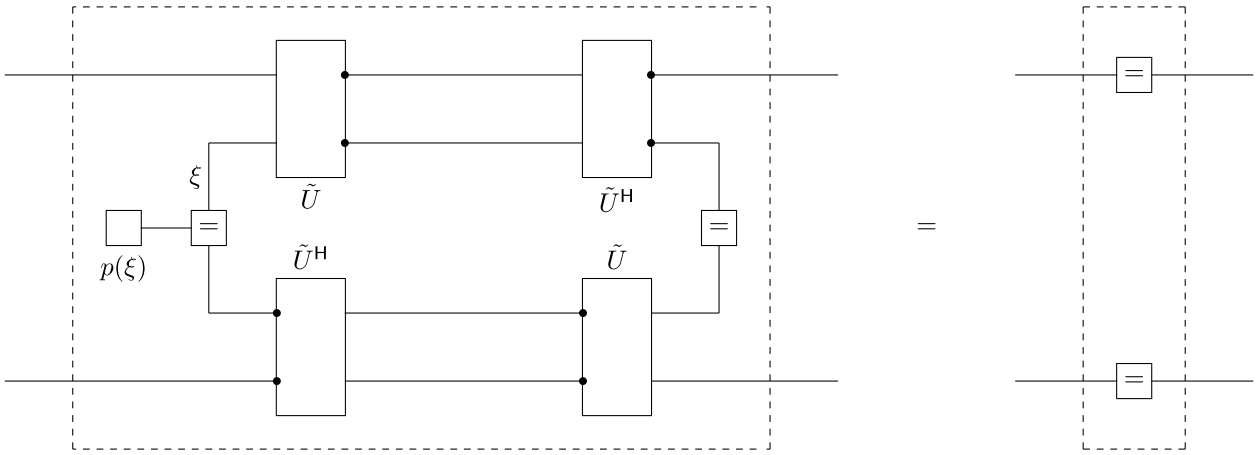

Fig. 21. Undoing a measurement as in Fig. 13.

in $\kappa_1, \ldots, \kappa_N$ as in Fig. 16, have the same effect as a single such interaction with

$$\kappa(\zeta, \zeta') = \prod_{\nu=1}^{N} \kappa_\nu(\zeta, \zeta'), \tag{45}$$

and due to (44), we generically[11] have

$$\lim_{N\to\infty} \prod_{\nu=1}^{N} \kappa_\nu(\zeta, \zeta') = f_{=}(\zeta, \zeta'). \tag{46}$$

In summary, the net effect of N marginalized unitary interactions as in Fig. 14 (left), in the limit $N \to \infty$, is a projection measurement. Such effects were studied, e.g., in [21].

C. Copying and Measurement by a Marginalized Copy

The circuit of Fig. 18 can be used to create (maximally entangled) copies of quantum variables: in any factor graph containing this circuit, both $\breve{X} = \tilde{X} = X$ and $\breve{X}' = \tilde{X}' = X'$ hold in all valid configurations.

Clearly, with multiple such circuits, any number of (maximally entangled) copies can be created, in principle up to macroscopic scale. However, if any such copy escapes to the environment (i.e., it is marginalized away), it effects a projection measurement of all the other copies, as illustrated in Fig. 19. It is thus obvious that large-scale copies of a quantum variable (a special case of a Schrödinger cat) are hard to maintain in a nonclassical state.

D. The Post-Measurement State and the Separation Condition

For the reductions in Figs. 13 and 14 to be correct, the measuring system (with variables ξ and $\tilde{\xi}$) must not again, directly or indirectly, interact with the system of interest (with variables X and X'):

Separation Condition (cf. Fig. 20): *After the measuring interaction, the measuring system does not interact with the system of interest throughout the period of interest.*

[11] We are here not concerned with the precise conditions for the validity of (46).

The separation need not hold forever, but it must hold *throughout the period of interest,* which ends with the terminating identity matrix in Figs. 20 and 8. After the period of interest, the measuring system may interact arbitrarily with the system of interest. (Recall that the terminating identity matrix summarizes arbitrary unitary evolutions, interactions, and measurements with unknown results.)

The standard post-measurement density matrix (as, e.g., in Fig. 7) is thus not unconditionally valid, but holds strictly only for a limited period of interest for which the Separation Condition holds.

If the Separation Condition is violated, the standard post-measurement density matrix is perhaps still a good approximation in most practical situations. However, if arbitrary post-measurement interactions are allowed, then measurements can be undone, as illustrated in Fig. 21. Such undoings are a key ingredient of the Frauchiger–Renner paradox, which will be discussed in the next section.

We have thus established that the Separation Condition is necessary and sufficient for the standard post-measurement density matrix to be entirely correct. However, the Separation Condition is not necessary for the existence of a classical measurement result (i.e., to effect an equality constraint between conjugate quantum variables). For example, if the measurement can be decomposed into two (or more) separate measurements as in Fig. 10 (left), it suffices if the Separation Condition applies to at least one of them.

Similarly, if the measurement is effected with multiple copies as in Section IV-C, it suffices if the Separation Condition holds for at least one copy. It is obvious that such measurements with a "macroscopic" number of copies are very robust and not easily undone.

V. The Frauchiger–Renner Paradox

We now turn to the Frauchiger–Renner paradox [15] and use it to illustrate many points of this paper. The reader need not be familiar with [15]: we give a complete description and analysis of the paradox in terms of factor graphs of quantum mass functions. If the reader is familiar with [15], he will notice that the perspectives of the different agents in [15] are here different marginals of a single quantum mass function. Technically, the results of our analysis agree with those in [15], except for the actual contradiction which involves classical variables that do not coexist (i.e., quantum variables that are not jointly classicable).

A. System Model and Factor Graphs

Factor graphs of the relevant quantum mass functions are given in Figs. 24–27, which represent the perspectives of Agents F, $\overline{\mathrm{W}}$, and W from [15], respectively. (The names of these agents as well as "Lab L" and "Lab $\overline{\mathrm{L}}$" are from [15]; otherwise, our notation differs from that in [15].) The overall (i.e., the most refined) factor graph that we will use is Fig. 27; Figs. 24, 25, and 26 are marginals of Fig. 27, as will be detailed below.

In these factor graphs, all variables are $\{0,1\}$-valued, except for Y_1, Y_1', $\breve{Y}_1$, which take values in $\{0,1,2,3\}$.

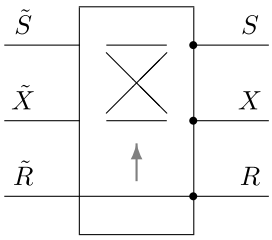

Fig. 22. Quantum-controlled swap function/matrix defined by (48) and (49).

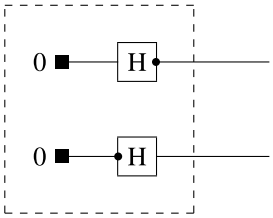

Fig. 23. The dashed box in Fig. 24 for $\breve{R} = 1$ (up to the scale factor $2/3$).

The rows and columns of all matrices are indexed beginning with 0. The nodes/boxes labeled "H" represent Hadamard matrices

$$H = \frac{1}{\sqrt{2}} \begin{pmatrix} 1 & 1 \\ 1 & -1 \end{pmatrix}. \tag{47}$$

We also use a quantum-controlled swap gate[12] (also known as Fredkin gate) as in Fig. 22. This function (or matrix) evaluates to 1 if either

$$R = \tilde{R} = 0 \text{ and } X = \tilde{X} \text{ and } S = \tilde{S} \tag{48}$$

or

$$R = \tilde{R} = 1 \text{ and } X = \tilde{S} \text{ and } S = \tilde{X}; \tag{49}$$

otherwise, it evaluates to zero. As a matrix, this function is unitary.

The matrix U is unitary with first column (the column with index 0) as in (56) below. (The second column is irrelevant.) The unitary matrix B will be discussed below. We now walk through these factor graphs one by one.

1) Fig. 24 — Lab $\overline{\mathrm{L}}$ and Agent F: The dashed box in Fig. 24 represents Lab $\overline{\mathrm{L}}$ of [15], which prepares the $\{0,1\}$-valued quantum variable S. The random bit $\breve{R}$ (with $\Pr(\breve{R} = 1) = 2/3$) results from measuring the quantum variable R. If $\breve{R} = 0$, then $S = S' = \breve{S} = 0$; if $\breve{R} = 1$, then the dashed box in Fig. 24 reduces to Fig. 23.

Agent F (in Lab L) measures S with result $\breve{S}$. Clearly,

$$\breve{S} = 1 \implies \breve{R} = 1. \tag{50}$$

2) Fig. 25 — Agent $\overline{W}$: Agent $\overline{\mathrm{W}}$ has unlimited quantum-level access to Lab $\overline{\mathrm{L}}$, but he has no access to S. In particular, he has access to the quantum variable X in Fig. 24 and he can undo the measurement of R (as in Fig. 21, not shown in Fig. 25). He then measures X and R jointly as shown in Fig. 25. The unitary matrix $B \in \mathbb{C}^{4\times 4}$ is chosen such that, first, ψ_{S,Y_1} (= the upper dashed box in Fig. 25) satisfies

$$\psi_{S,Y_1}(0,0) = 0, \tag{51}$$

[12]There is no controlled-swap gate in [15]. We use it to make the analysis more transparent.

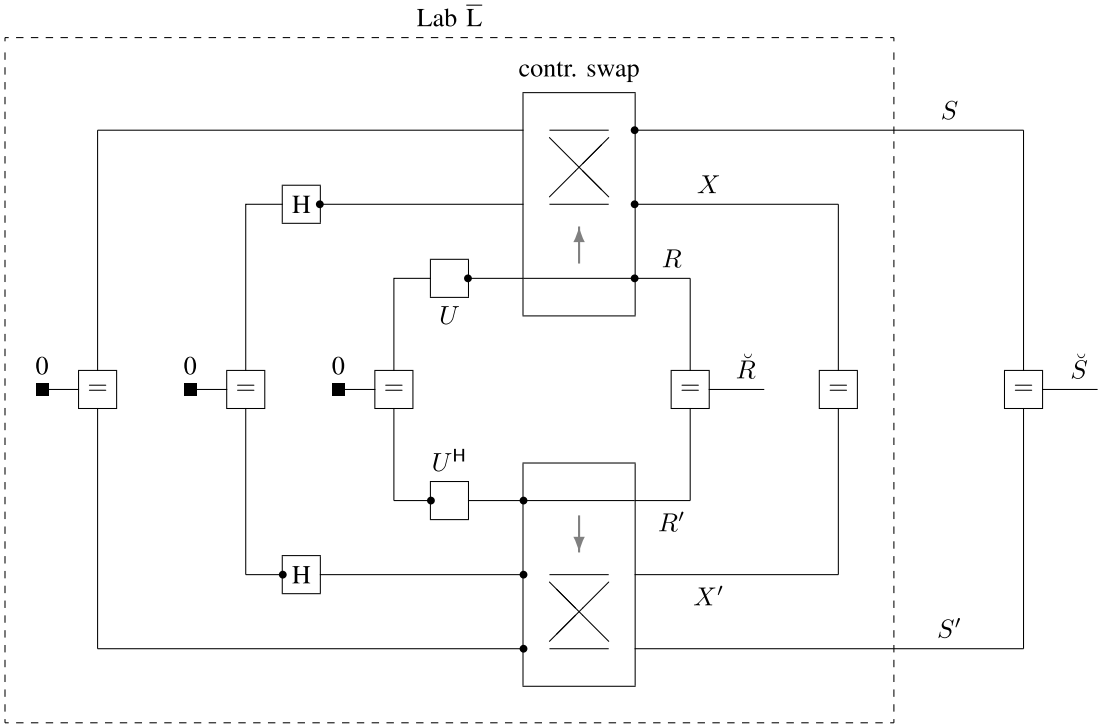

Fig. 24. The first step in the Frauchiger–Renner Gedankenexperiment: the view of Agent F.

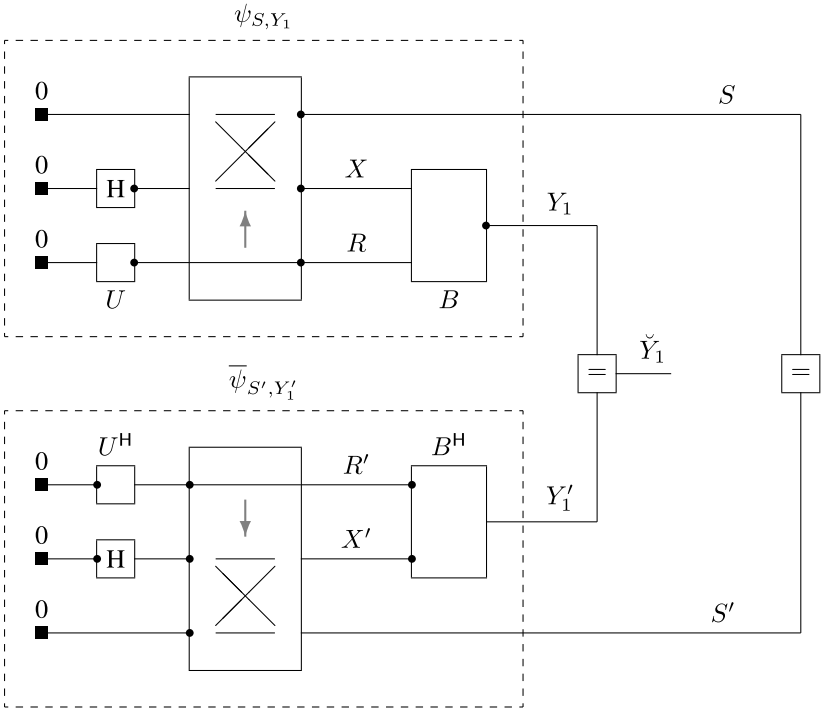

Fig. 25. The view of Agent $\overline{\mathrm{W}}$. The unitary transform B is chosen such that (51) and (54) are satisfied.

and second, that (54) holds. A possible choice of the first row of such a matrix is given in (58). (The other rows of B are irrelevant.) The verification of B having the required properties is given in Section V-C.

From (51) and its mirror equation $\overline{\psi}_{S',Y_1'}(0,0) = 0$, we have

$$\breve{Y}_1 = 0 \implies S = S' = 1. \tag{52}$$

3) Fig. 26 — Agent W: Agent W has unlimited quantum-level access to Lab L, the lab of Agent F (but no access to Lab $\overline{\mathrm{L}}$). In particular, he can undo the measurement of S (not shown in Fig. 26). He then measures S as shown in Fig. 26. From Fig. 26, it is easily seen that

$$\breve{R} = 1 \implies \breve{Y}_2 = 0. \tag{53}$$

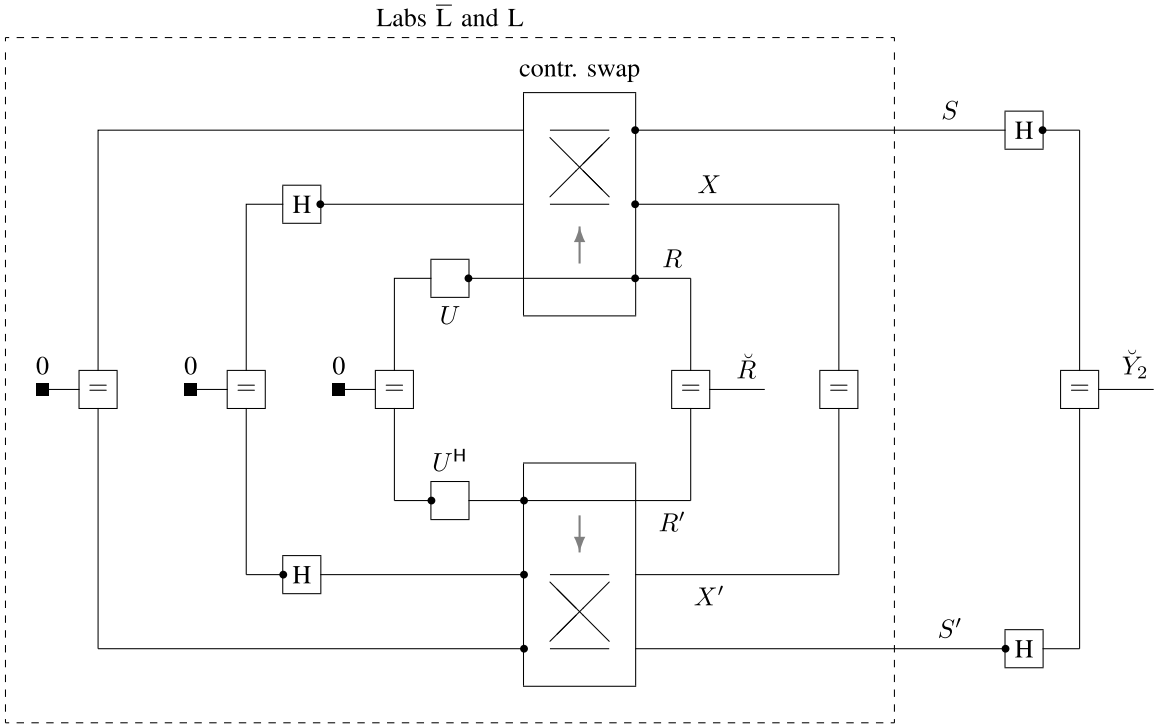

Fig. 26. The view of Agent W.

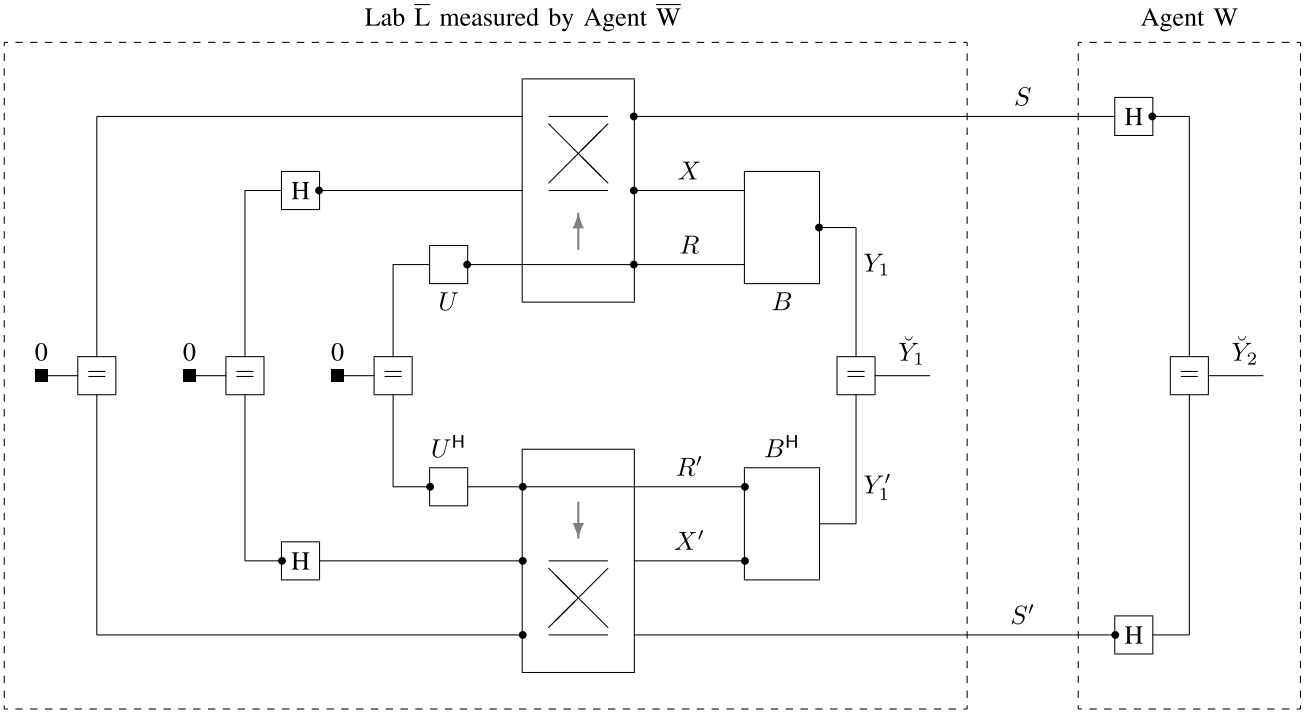

Fig. 27. Factor graph of the entire Frauchiger–Renner model [15]. In the notation of this paper, the condition for the paradox (the stopping condition in [15]) is $\breve{Y}_1 = 0$ and $\breve{Y}_2 = 1$.

4) Fig. 27 — The Entire Model: Fig. 27 shows the quantum mass function of the entire model. Note that Figs. 24, 25, and 26 are marginals of Fig. 27. We also note that

$$\Pr(\breve{Y}_1 = 0 \text{ and } \breve{Y}_2 = 1) > 0, \tag{54}$$

as shown in Section V-C.

B. The Paradox

Suppose we observe $\breve{Y}_1 = 0$ and $\breve{Y}_2 = 1$ (which is possible by (54), see also (59)). Using (52), the measurement of S as in (50), and (53), we have

$$\breve{Y}_1 = 0 \implies \breve{S} = 1 \implies \breve{R} = 1 \implies \breve{Y}_2 = 0, \tag{55}$$

which contradicts the observation $\breve{Y}_2 = 1$.

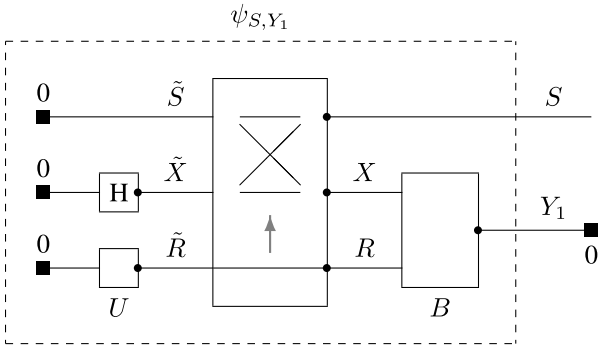

Fig. 28. A critical function/box in the Frauchiger–Renner model.

TABLE I
THE VALID CONFIGURATIONS IN FIG. 28 AND THEIR FUNCTION VALUE

R	$\tilde{R}$	X	$\tilde{X}$	S	$\tilde{S}$	function value: symbolic	function value: numerical
0	0	0	0	0	0	$u_0 b_{R,X}(0,0)\frac{1}{\sqrt{2}}$	$\frac{1}{2\sqrt{6}}$
0	0	1	1	0	0	$u_0 b_{R,X}(0,1)\frac{1}{\sqrt{2}}$	$\frac{1}{2\sqrt{6}}$
1	1	0	0	0	0	$u_1 b_{R,X}(1,0)\frac{1}{\sqrt{2}}$	$\frac{-1}{\sqrt{6}}$
1	1	0	1	1	0	$u_1 b_{R,X}(1,0)\frac{1}{\sqrt{2}}$	$\frac{-1}{\sqrt{6}}$

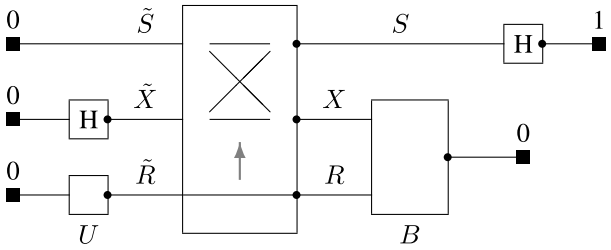

Fig. 29. An extension of Fig. 28.

TABLE II
THE VALID CONFIGURATIONS IN FIG. 29 AND THEIR FUNCTION VALUES

R	$\tilde{R}$	X	$\tilde{X}$	S	$\tilde{S}$	function values: symbolic	function values: numerical
0	0	0	0	0	0	$u_0 b_{R,X}(0,0)\frac{1}{2}$	$\frac{1}{4\sqrt{3}}$
0	0	1	1	0	0	$u_0 b_{R,X}(0,1)\frac{1}{2}$	$\frac{1}{4\sqrt{3}}$
1	1	0	0	0	0	$u_1 b_{R,X}(1,0)\frac{1}{2}$	$\frac{-1}{2\sqrt{3}}$
1	1	0	1	1	0	$-u_1 b_{R,X}(1,0)\frac{1}{2}$	$\frac{1}{2\sqrt{3}}$

The paradox is resolved by noting that the three implications in (55) do not hold simultaneously: the quantum variables R, S, Y_1, and Y_2 are not jointly classicable, i.e., $\breve{R}$, $\breve{S}$, $\breve{Y}_1$, and $\breve{Y}_2$ do not coexist in any common scope. (Assumption C of [15] presumes such variables to exist absolutely and does not hold in this paper.)

C. The Details

1) The Matrices U and B: The unitary matrices U and B can be chosen as follows. (The choices below replicate the settings of [15], but other choices are possible.) The first column (the column with index 0) of U is defined to be

$$(u_0, u_1)^{\mathsf{T}} = \big(\sqrt{1/3}, \sqrt{2/3}\big)^{\mathsf{T}}. \tag{56}$$

The other columns of U are irrelevant. The first row (the row indexed by $Y_1 = 0$) of B is defined to be

$$b = \big(b_{R,X}(0,0), b_{R,X}(0,1), b_{R,X}(1,0), b_{R,X}(1,1)\big) \tag{57}$$

$$= (1/2, 1/2, -\sqrt{1/2}, 0). \tag{58}$$

The other rows of B are irrelevant.

2) Fig. 28 and Condition (51): We next examine Fig. 28, which is a critical block of (our factor graph representation of) the Frauchiger–Renner model, cf. Fig. 25. The valid configurations in Fig. 28 with fixed $Y_1 = 0$ are listed in Table I, each with the resulting function value (i.e., the product of all factors in Fig. 28).

Now let ψ_{S,Y_1} be the exterior function of the dashed box in Fig. 28. Noting that $\psi_{S,Y_1}(0,0)$ is the sum of the function values of the first three lines in Table I, we obtain (51).

3) Fig. 29 and Condition (54): It remains to prove (54). To this end, we need the extension of Fig. 28 shown in Fig. 29. The valid configurations and their function values are listed in Table II, which is easily obtained from Table I. The sum of these function values[13] is $\frac{1}{2\sqrt{3}}$, from which we obtain

$$\Pr(Y_0 = 0 \text{ and } Y_1 = 1) = 1/12 \tag{59}$$

in Fig. 27, in agreement with [15].

VI. CONCLUSION

Using quantum mass functions, we have discussed the realization of projection measurements as marginalized unitary interactions. It follows that classical measurement results strictly belong to *local* models, i.e., marginals of more detailed models. Different marginals of the same model may have incompatible classical variables. The pertinent compatibility (or incompatibility) is characterized by the notion of joint classicability. For illustration, we have used the Frauchiger–Renner paradox, which yields "contradictory" classical variables that do not coexist.

ACKNOWLEDGMENT

The helpful comments by R. B. Griffiths, J. B. Hartle, and C. Taubes, and the anonymous reviewers are gratefully acknowledged.

REFERENCES

[1] J. A. Wheeler and W. H. Zurek, Eds., *Quantum Theory and Measurement*. Princeton, NJ, USA: Princeton Univ. Press, 1983.
[2] W. H. Zurek, "Quantum darwinism," *Nature Phys.*, vol. 5, pp. 181–188, Mar. 2009.

[13] i.e., the partition sum of Fig. 29 [8]

[3] W. H. Zurek, "Decoherence, einselection, and the quantum origins of the classical," *Rev. Mod. Phys.*, vol. 75, no. 3, pp. 715–775, Jul. 2003.
[4] H.-P. Breuer and F. Petruccione, *Open Quantum Systems*. New York, NY, USA: Oxford Univ. Press, 2002.
[5] M. Schlosshauer, "Decoherence, the measurement problem, and interpretations of quantum mechanics," *Rev. Mod. Phys.*, vol. 76, pp. 1267–1305, Feb. 2004.
[6] A. A. Clerk, H. M. Devoret, S. M. Girvin, F. Marquardt, and R. J. Schoelkopf, "Introduction to quantum noise, measurement, and amplification," *Rev. Mod. Phys.*, vol. 82, pp. 1155–1208, Apr./Jun. 2010.
[7] A. E. Allahverdyan, R. Balian, and T. M. Nieuwenhuizen, "Understanding quantum measurement from the solution of dynamical models," *Phys. Rep.*, vol. 525, no. 1, pp. 1–166, Apr. 2013.
[8] H.-A. Loeliger and P. O. Vontobel, "Factor graphs for quantum probabilities," *IEEE Trans. Inf. Theory*, vol. 63, no. 9, pp. 5642–5665, Sep. 2017.
[9] M. Gell-Mann and J. B. Hartle, "Quantum mechanics in the light of quantum cosmology," in *Proc. Santa Fe Inst. Workshop Complex., Entropy, Phys. Inf.*, May 1989. [Online]. Available: https://arxiv.org/abs/1803.04605
[10] H. F. Dowker and J. J. Halliwell, "Quantum mechanics of history: The decoherence functional in quantum mechanics," *Phys. Rev. D, Part. Fields*, vol. 46, pp. 1580–1609, Aug. 1992.
[11] R. B. Griffiths, *Consistent Quantum Theory*. Cambridge, U.K.: Cambridge Univ. Press, 2002.
[12] R. Penrose, "Applications of negative dimensional tensors," in *Combinatorial Mathematics and Its Applications*. New York, NY, USA: Academic, 1971.
[13] C. J. Wood, J. D. Biamonte, and D. G. Cory, "Tensor networks and graphical calculus for open quantum systems," *Quantum Inf. Comput.*, vol. 15, nos. 9–10, pp. 759–811, 2015.
[14] C. M. Caves, "Quantum mechanics of measurements distributed in time. A path-integral formulation," *Phys. Rev. D, Part. Fields*, vol. 33, pp. 1643–1665, Mar. 1986.
[15] D. Frauchiger and R. Renner, "Quantum theory cannot consistently describe the use of itself," *Nature Commun.*, vol. 9, Sep. 2018, Art. no. 3711.
[16] (Sep. 2018). *Blog of Scott Aaronson*. [Online]. Available: https://www.scottaaronson.com/blog/?p=3975
[17] D. Lazarovici and M. Hubert, "How quantum mechanics can consistently describe the use of itself," *Sci. Rep.*, vol. 9, Jan. 2019, Art. no. 470.
[18] H.-A. Loeliger, "An introduction to factor graphs," *IEEE Signal Process. Mag.*, vol. 21, no. 1, pp. 28–41, Jan. 2004.
[19] M. X. Cao and P. O. Vontobel, "Double-edge factor graphs: Definition, properties, and examples," in *Proc. IEEE Inf. Theory Workshop*, Kaohsiung, Taiwan, Nov. 2017, pp. 136–140.
[20] M. A. Nielsen and I. L. Chuang, *Quantum Computation and Quantum Information*, 10th ed. Cambridge, U.K.: Cambridge Univ. Press, 2010.
[21] M. Bauer, D. Bernard, and T. Benoist, "Iterated stochastic measurements," *J. Phys. A, Math. Theor.*, vol. 45, no. 49, 2012, Art. no. 494020.

Hans-Andrea Loeliger (S'85–M'92–SM'03–F'04) received the Diploma degree in electrical engineering from ETH Zürich. In 1992, he received the Ph.D. degree from ETH Zürich. From 1992 to 1995, he was with Linköping University, Sweden. From 1995 to 2000, he was a full-time Technical Consultant and a Co-Owner of a consulting company. Since 2000, he has been a Professor with ETH Zürich. His research interests have been in the broad areas of signal processing, machine learning, information theory, quantum systems, error correcting codes, communications, electronic circuits, and neural computation.

Pascal O. Vontobel (S'96–M'97–SM'12) received the Diploma degree in electrical engineering, the Post-Diploma degree in information techniques, and the Ph.D. degree in electrical engineering from ETH Zürich, Switzerland, in 1997, 2002, and 2003, respectively.

From 1997 to 2002, he was a Research and a Teaching Assistant with the Signal and Information Processing Laboratory, ETH Zürich. Besides this, he was a Post-Doctoral Research Associate with the University of Illinois at Urbana–Champaign from 2002 to 2004, a Visiting Assistant Professor with the University of Wisconsin–Madison from 2004 to 2005, a Post-Doctoral Research Associate with the Massachusetts Institute of Technology in 2006, and a Visiting Scholar with Stanford University in 2014. From 2006 to 2013, he was a Research Scientist with the Information Theory Research Group, Hewlett–Packard Laboratories, Palo Alto, CA, USA. Since 2014, he has been an Associate Professor with the Department of Information Engineering, The Chinese University of Hong Kong. His research interests lie in coding and information theory, quantum information processing, data science, communications, and signal processing.

Dr. Vontobel has been an Associate Editor for the IEEE TRANSACTIONS ON INFORMATION THEORY (2009–2012), an Awards Committee Member of the IEEE Information Theory Society (2013–2014), a Distinguished Lecturer of the IEEE Information Theory Society (2014–2015), and an Associate Editor for the IEEE TRANSACTIONS ON COMMUNICATIONS (2014–2017). Moreover, has been a TPC co-chair of the 2016 IEEE International Symposium on Information Theory, the 2018 IEICE International Symposium on Information Theory and its Applications, and the 2018 IEEE Information Theory Workshop, along with co-organizing several topical workshops and being on the technical program committees of many international conferences. Moreover, he has been three times a plenary speaker at international information and coding theory conferences, he has received an exemplary reviewer award from the IEEE Communications Society, and has been awarded the ETH medal for his Ph.D. dissertation.